

Decadal variability in the Southern Hemisphere

Xiaojun Yuan¹ and Emmi Yonekura²

Received 21 January 2011; revised 20 June 2011; accepted 28 June 2011; published 13 October 2011.

[1] This study reveals that a quasi-decadal variability exists in the climate system of southern high latitudes, particularly in the Southern Annular Mode (SAM) and subpolar to mid latitudes sea surface temperature (SST), based on in situ observations, reanalysis data, and the 20th Century runs of IPCC AR4 coupled climate models. Spectral analysis reveals that a statistically significant variability with periods of 8–16 years appears in the SAM indices based on about 50 years of reanalysis data and observed SST. Observations of air temperature and sea level pressure from weather stations confirm that the decadal variability is more evident in the midlatitudes than over Antarctica. Cross-spectral analysis indicates that the SAM index is related to the SST in the subpolar seas of Antarctica and SST gradient at mid-high latitudes at this decadal frequency band. The SAM indices from 20th century runs (longer than 100 years) of eighteen IPCC coupled climate models are also examined for the decadal variability. Sixteen out of the eighteen models exhibit decadal variability in SAM that is significant at least at the 90% of confidence level while eight are significant at the 95% confidence level. Seven models produce significant co-variability between SAM and subpolar SST at this quasi-decadal frequency.

Citation: Yuan, X., and E. Yonekura (2011), Decadal variability in the Southern Hemisphere, *J. Geophys. Res.*, 116, D19115, doi:10.1029/2011JD015673.

1. Introduction

[2] Regional decadal and multidecadal variabilities in the Southern Hemisphere have been investigated for the Australian/Southeast Indian Ocean/Southwest Pacific Ocean region [Allan and Haylock, 1993], for the South Indian Ocean [Allan *et al.*, 1995], for the Southeast Pacific region [Salinger *et al.*, 1996] and for the South Atlantic [Venegas *et al.*, 1996]. Reason [2000] examined the multidecadal (every twenty years) variability in sea surface temperature (SST), air temperature, surface wind stress in the Southern Hemisphere from the tropics to mid altitudes. His results suggest that the dynamic effect from surface wind stress anomalies plays an important role in the regions with major current systems while the thermodynamic effect is a key factor influencing the SST variability in most subtropics and mid latitudes at this time scale.

[3] In the southern subpolar ocean, our knowledge regarding the decadal variability in the southern hemisphere mostly comes from investigations of the El Niño/Southern Oscillation (ENSO) teleconnection. For the last few decades, the relationships between precipitation and moisture fluxes in the western Antarctic and ENSO variability have changed from out-of-phase in 1980s to in phase in 1990s

[Cullather *et al.*, 1996; Bromwich *et al.*, 2000, 2004]. Fogt and Bromwich [2006] described this decadal change in terms of the general circulation as depicted in correlations between ENSO index and sea level pressure (SLP). They attribute the amplified ENSO response in high latitudes during the 1990s to the fact that the Southern Annular Mode (SAM) is out-of-phase with ENSO in the 1980s but in phase with ENSO in the 1990s, which enhances the ENSO signal in high latitudes. Stammerjohn *et al.* [2008] support their argument by showing that the faster sea ice retreat west of the Antarctic Peninsula is due to the in-phase effect from cold ENSO events and positive SAM during 1990s, which didn't occur in 1980s. Such change implies a possible regime shift at the time scale of a decade or longer. In Australia, rainfall records show considerable decadal variability that can be linked to SAM variability [Meneghini *et al.*, 2007]. For longer time periods, Villalba *et al.* [1997] reconstruct the summer trans-polar index, which measures the eccentricity of the polar vortex [Pittock, 1980], by using SLP proxy data built by subantarctic tree ring records in South America and Hobart, Australia. They find that the trans-polar-index with a record length of 119 years is related to ENSO variability at decadal frequency (14-year period) as revealed in the coherence spectrum. The question is whether this ENSO teleconnection-related decadal variability is originated from the high latitudes or the tropics? In other words, is there natural variability in the atmospheric circulation of southern high latitudes that is readily interactive with the ENSO signal at a decadal time scale?

¹Lamont-Doherty Earth Observatory of Columbia University, Palisades, New York, USA.

²Department of Earth and Environmental Sciences, Columbia University, New York, New York, USA.

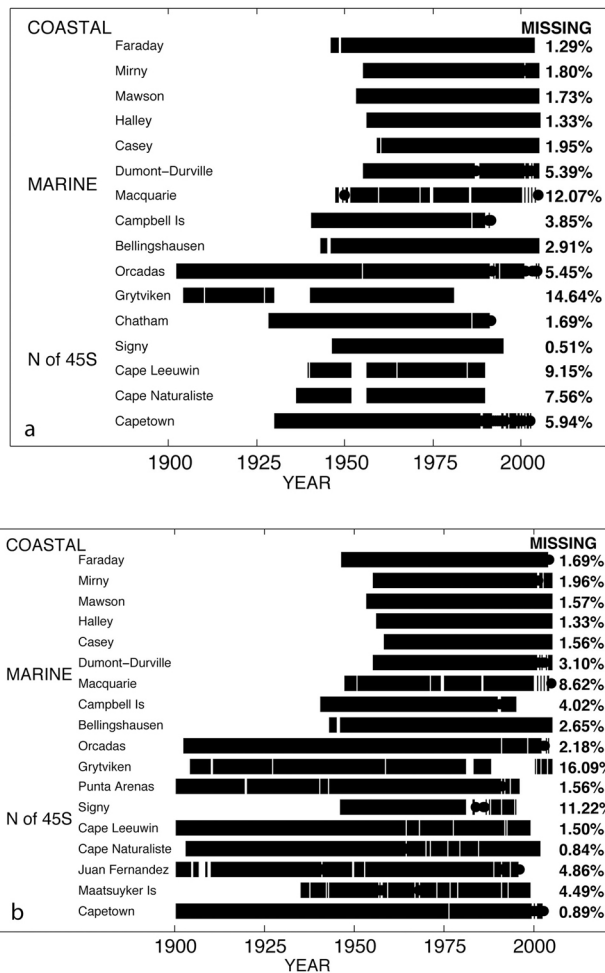


Figure 1. Weather station data coverage for (a) sea level pressure and (b) surface air temperature. The percentage of missing data for each station is listed at right.

[4] SAM is a major climate mode in the atmospheric pressure field linking mid latitudes to the polar region of the Southern Ocean [Gong and Wang, 1999; Thompson and Wallace, 2000; Simmonds, 2003]. Our recent study [Yuan and Li, 2008] suggests that a decadal variability likely exists in SAM. In the study, we systematically examine the cross-relationships of four climate modes: Pacific South America pattern (PSA), stationary wave number-3 pattern (Wave-3), SAM, and Semi-annual Oscillation (SAO). The highest energy peak of each cross-spectra between SAM and the other three modes all occurs at the decadal frequency band and all are significant at the 95% confidence level. The highest energy peak of each cross-spectra of wave3 vs SAO, wave3 vs PSA and SAO vs PSA (no SAM involved) does not occur at decadal frequency bands. There is no decadal peak in the cross-spectrum between PSA and wave3. The decadal peaks in the cross-spectra of SAO vs PSA and SAO vs wave3 never become significant at the 95% confidence level [Yuan and Li, 2008, Figure 5]. The study suggests the possibility of a high-latitude originated decadal variability. Here we show that the decadal variability is a statistically robust phenomenon in the climate system of the

southern extratropics, which can be found in over 50 years instrumental data, reanalysis data and in the twentieth century runs of the coupled climate models.

2. Data and Method

[5] We use three types of data sets in this study. The first type is instrumental data. We select weather stations in the southern ocean with records close to 50 years and longer from the Reference Antarctic Data for Environmental Research (READER) database [Turner *et al.*, 2005]. Eighteen stations with record length ranging from 47 to 103 year are selected (Figure 1). They are classified as Antarctic coastal, subpolar marine and midlatitude (north 45°S) stations. Most stations have a few percent of data gaps in their monthly temperature and pressure records, which are filled by the climatology at each station. In general, temperature records are usually longer and have fewer gaps than the pressure records at these stations. In addition, we include two observation-based SAM indices: monthly series from British Antarctic Survey [Marshall, 2003] and yearly series provided by Dr. Visbeck from Kiel University [Visbeck, 2009]. The sea surface temperature (SST) with one-degree resolution from Hadley Centre sea ice and SST data set for the period of 1950 to 2004 [Rayner *et al.*, 2003, Hurrell *et al.*, 2008] are also used. The second type contains reanalysis data sets, including National Centers for Environmental Prediction (NCEP)-National Center for Atmospheric Research (NCAR) reanalysis from 1950 to 2004 [Kalnay *et al.*, 1996; Kistler *et al.*, 2001], and ERA-40 from 1957 to 2001 [Uppala *et al.*, 2005]. Since this study focuses on low frequency variability in the atmosphere and ocean, the existing data problems in NCEP/NCAR reanalysis in the southern ocean [Kistler *et al.*, 2001] are not critical to our analysis and results. Finally, we examine sea level pressure (SLP) and SST from the 20th century runs of 18 coupled climate models from Intergovernmental Panel on Climate Change (IPCC) Climate Model Inter-comparison Program. The 20th century runs from all models have output longer than 100 years. The length of time series from each model can be found in Table 3.

[6] A SAM index has been defined in a number of ways in earlier studies: the difference between zonal mean SLP at 40°S and 65°S [Gong and Wang, 1999] or the principal component of leading EOF mode of SLP [Rogers and van Loon, 1982; Yuan and Li, 2008] or geopotential height at 850mb [Thompson and Wallace, 2000], and 500mb [Rogers and van Loon, 1982; Kidson, 1999]. The spatial patterns from all these SAM indices are quite similar: an annular shape around the Antarctic with an opposite phase of pressure or height anomaly in the polar and mid latitude regions. It represents a largely symmetric atmospheric mass seesaw between mid latitudes and the Antarctic continent. This zonally symmetric pattern usually breaks west of Antarctic Peninsula to the Amundsen Sea where polar pressure anomaly extends further north and weakens the mid latitude pressure anomaly. The key centers of PSA and SAM are both located in the Amundsen/Bellingshausen Sea region [Simmonds and King, 2004, Turner *et al.*, 2009]. This zonal asymmetry of SAM likely reflects shared variance and/or interaction between ENSO and SAM at inter-annual time scales. Modified from Gong and Wang [1999], we define the SAM index as differences of monthly SLP

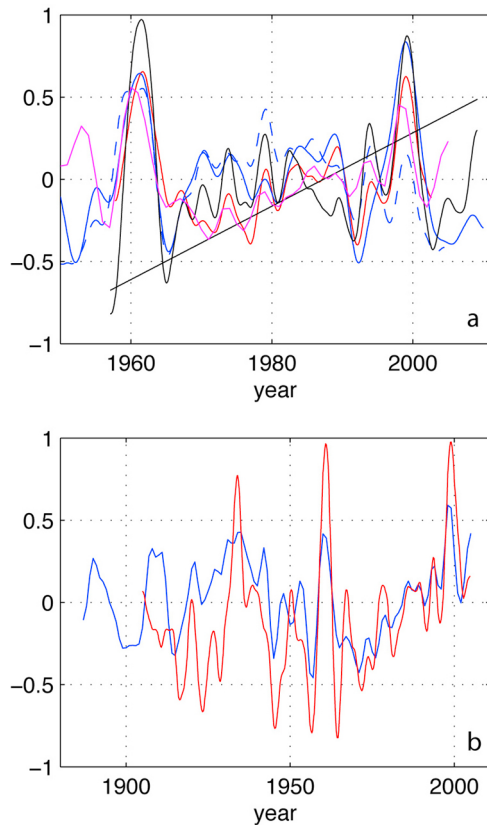


Figure 2. (a) Detrended SAM indices from BAS (black), Visbeck (magenta), ERA40 (red), NCEP (blue) and NCEP-EOF (blue dash line) after 1950. Black straight line is the long-term trend removed from the BAS series. (b) Reconstructed Visbeck annual SAM series (blue) and Fogt seasonal SAM series since 1905 (red). All time series were filtered by a butterworth filter with the filter width of 5 years.

anomalies between 40°S and 65°S in this study. The modification is that we use SLP anomaly instead of mean SLP. The mean SLP climatology at southern mid and high latitudes exhibits a strong semiannual and seasonal variation. Using SLP anomaly effectively reduces the influence of seasons and SAO, and allows us focus on the SAM variability. The leading EOF modes of monthly mean SLP and SLP anomalies have 30% and 28% of variance of their time series, respectively. The former contains more seasonal and semi-annual variability. The eigenvectors of these two leading modes are very similar with a spatial correlation of 0.60. In addition, two reconstructed SAM indices from Visbeck [2009] and Fogt *et al.* [2009a] are considered too. Both reconstructions are based on weather station data and extended back to the 19th century.

[7] We use power spectrum analysis extensively in this study. To focus on the decadal variability, the long-term trend is removed from all time series prior to the spectral analysis. Spectral analysis is then applied to unfiltered but standardized time series. However, we smooth the spectral power by a three-point running mean filter in the frequency domain to reduce the uncertainty of energy peaks [Priestley, 1992] when a monthly time series is used. Such practice is

not applied to yearly time series because of limited resolution in frequency. Our calculation shows that the SAM is an order 6 autoregressive process. Spectra peaks are then assessed by first order Markov null continuum method. We generate 200 noise series from AR(1) process that retain the lag-1 autocorrelation in original SAM time series. The significance level is determined by comparing the spectra power from the original time series with powers from the 200 random series at each frequency band. It reveals the confidence level that the periodicity at a certain frequency is significantly different than none periodicity process of AR(1). In addition, we apply short-time Fourier transform and examine the spectral power as functions of frequency and time. A 50-year window is chosen and slid along the entire time series at a 5-year interval. We then calculate power spectra from each short series and create spectrogram as a function of frequency and center year of each 50-year segment. It reveals how the spectral power changes over the time.

3. Decadal Variability of SAM

[8] SAM indices based on the modern instrumental data and reanalysis data are displayed in Figure 2a. Most indices are based on the differences of normalized SLP anomalies between 40°S and 65°S with a couple of exceptions. The dashed blue line is the principal component of leading EOF mode of NCEP/NCAR SLP anomaly. After removing the long-term trend, the most striking and consistent feature from these time series is the two large positive anomalies centered in the early 1960s and late 1990s. Accompanying these two positive anomalies are relatively large negative anomalies before and after the positive peaks. A cycle of these large anomalies lasts slightly longer than a decade. The amplitude of changes from positive peak to negative peak within such a cycle is equivalent to the total change of the long-term trend during the last 53 years as marked by the black straight line based on observations [Marshall, 2003]. Outside of these two groups of large swinging anomalies, SAM indices are weakly positive or negative between 1970 and 1990. The consistent feature of most SAM indices is these two large amplitude events separated by about 30 years superimposed on the oscillatory variability with lower amplitudes at interannual and decadal time scales. This common feature suggests amplified forcing or stronger variability at a multidecadal scale.

[9] Even though most SAM indices reveal the common feature of low frequency variability at multidecadal scales, there are many differences among the indices due to the spatial and temporal coverage of different data sets as well as differences in simulation models. The differences are particularly profound during weak SAM phase (1970–1990). For example, Visbeck and BAS SAM indices are both based on data from weather stations. However, they used two different sets of weather stations, which resulted in the differences in their SAM indices (magenta and black lines). Differences in SAM indices also come from different definitions. Defined by latitude differences and EOF leading mode, NCEP/NCAR reanalysis data yield different SAM indices (blue solid and blue dashed line). The EOF based SAM index misses the large positive anomaly in 1990. The cross-correlations among these indices are given in Table 1.

Table 1. Cross-Correlation Coefficients Among SAM Indices Derived From Different Data Sources^a

Data Sets and Time Span	Visbeck	BAS	NCEP	ERA40
Visbeck (1880–05)	1			
BAS (57–08)	0.83 (49)	1		
NCEP (49–09)	0.67 (53)	0.81 (57)	1	
ERA40 (8/57–8/02)	0.84 (43)	0.77 (43)	0.85 (43)	1

^aThe lengths of correlating series in years are in brackets.

These indices are not perfectly correlated, reflecting above differences, but they share a large amount of variance. Following each of these SAM indices, there are positive peaks in approximately every five years and every ten years. These humps and valleys are consistent in phase even though the magnitudes vary, indicating consistent oscillatory behavior at interannual and decadal time scales. In addition, magnitudes of trends in these SAM indices are also quite different, although they are all positive (not shown here). That is not a surprise because of variable trends existing in mid-high latitudes of Southern Ocean from different reanalyses [Bromwich *et al.*, 2007]. Marshall [2003] showed that NCEP/NCAR reanalysis over-estimate SAM's trend by 2 times comparing to station data based SAM index.

[10] Since instrumental data periods are rather short for investigating decadal variability, we also examine two observations-based reconstructions of SAM indices longer

than 100 years. Visbeck [2009] reconstructed a proxy SAM index back to the 1880s, based on atmospheric mass conservation between the polar region and mid latitudes. Another proxy SAM index was created by Fogt [Jones *et al.*, 2009; Fogt *et al.*, 2009a] using the method of principal component regression to hindcast SLP back to 1865. Fogt's SAM index use the BAS SAM index as a predictant. Figure 2b shows the Visbeck and Fogt SAM time series. Fogt's SAM is only plotted from 1905 since there are missing data in the early years that interfere with filtering. Both reconstructed indices show the large amplitudes in early 1960s and late 1990s. The large amplitude anomaly swings shown in Figure 2a occurred in the early twentieth century too (Figure 2b). Multidecadal changes also exist at 20–30 years time scales. Fogt's SAM exhibits stronger oscillatory behavior at the decadal time scale.

[11] It is noted that the long-term trend is not removed from Visbeck's SAM, while it is removed from SLP before the reconstruction of Fogt SAM. Clearly there is a strong upward trend in the late twentieth century but also a decreasing trend between the 1930s and early 1950s in both Visbeck and Fogt SAMs. However, the total trend in Visbeck SAM since the 1880s is rather small. The modern time upward trend in SAM since the 1970s could be partially caused by this natural variability at multidecadal time scales.

[12] These quasi-decadal variations in SAM can be picked up by spectrum analysis. Figure 3a shows the power spectral

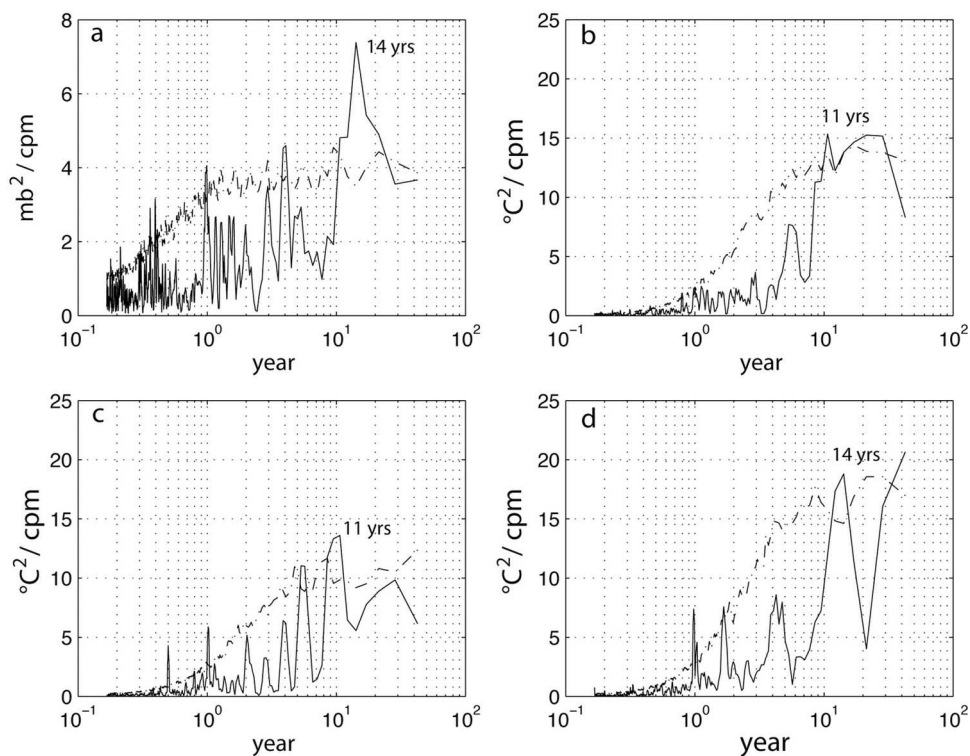


Figure 3. (a) Power spectrum density of the SAM EOF-based index constructed from 55 years of NCEP/NCAR monthly SLP anomaly. The dotted-dashed line indicates the 95% confidence level based on the red noise bootstrap significance test. The decadal peak in SLP anomaly differences-based SAM index is also significant at 95% confidence level. Power spectrum density of zonal mean SST anomalies in (b) 30°S–40°S, (c) 40°S–50°S, and (d) 50°S–60°S latitude bands. Again dotted-dashed lines mark the 95% confidence level.

Table 2. Significance Levels of Decadal Peaks and Associated Periods (in Bracket) in Observations

Seasons	BAS - 53 yrs	Visbeck - 119 yrs	Regions	Visbeck - 119 yrs
Spring	95 (8)	90 (12.8)	S. American	95 (16)
Summer	95 (9)	90 (8.5)	New Zealand/Australia	90 (16)
Fall	95 (16)	95 (18)	South Africa	90 (10)
Winter	95 (9)	95 (8.3)	Antarctic	90 (11.6)

density of the SAM index from NCEP/NCAR reanalysis data, which peaks near the 14 years period and stands above the 95% confidence level. It is consistent with SAM associated cross-spectrum in instrumental data periods [Yuan and Li, 2008, Figure 5] and also consistent with peak frequency in the summer trans-polar index derived from over 230 years of tree ring data [Villalba *et al.*, 1997]. Since spectrum analysis is sensitive to the length of the time series and the width of anomalies, distributions of power spectra density vary among SAM indices in Figure 2a. Based on monthly time series, both SAM indices from NCEP/NCAR reanalysis have significant peaks (95% confidence level) at periods of 14 years, while ERA40 (difference based) SAM index has significant (90% confidence level) energy peak at period of 10.6 years. The decadal peak in monthly BAS index does not exceed the 90% confidence level. However, some consistent patterns emerge when we examine the yearly time series as a function of seasons and regions (Table 2). From winter to summer, BAS SAM index yield significant (at 95% confidence level) peaks at periods of 8–9 years. In the fall, it yields a significant peak (95% confidence level) at 16 years period. The seasonal energy peaks in Visbeck SAM index occur at periods from 8 to 18 years. In addition, the Pan Pacific region (including South America and Australia/New Zealand) exhibits most significant decadal variability at the period of 16 years, while the decadal peaks in South Africa and Antarctica have relatively lower confidence levels (Table 2).

[13] To examine how stable the decadal variability is in longer time series, we conduct the spectral analysis of Fogt SAM index of 150 years. The missing data before 1905 (mostly in winter) are set to zero, which is equivalent to setting the missing pressure records to climatology. The power spectrum reveals three energy peaks at 6.7 years, 9.5 years and 23 years, which are all significant at the 95% confidence level (Figure 4a). Clearly decadal to multi-decadal oscillations are important variability in this long series. The spectrogram of the SAM index (Figure 4b) also reveals that the decadal variability is more prominent after 1915 (since center year of 1940) at relatively consistent periods of 7–9 years. The multidecadal variability started early (center year of 1910) but does not last after 1975. The method cannot resolve multidecadal variability with periods longer than 25 years.

4. Decadal Variability in the Southern Ocean

[14] To assess the robustness of the decadal variability in these SAM indices and also to isolate where the decadal variability is more profound, we examine the surface air temperature and pressure records from weather stations. Power spectrum analysis is applied to each temperature and pressure anomaly series at each of the eighteen weather stations. We mark significant decadal (periods of 8–16 years)

and interannual (periods of 3–7 years) variabilities in pressure and temperature records in Figure 5. Most decadal variability in pressure records occurs in the mid latitude oceans and continents, as well as in the stations on the Antarctic Peninsula, which are further north than other Antarctic coastal stations (Figure 5b). Only one Antarctic coastal station (Mawson) other than the stations on the Peninsula exhibits the decadal variability. However, the interannual variability is found in most stations from mid latitudes to the Antarctic coast. The temperature records exhibit more significant decadal and interannual variability than the pressure records: the decadal variability mostly occurs in mid latitudes and the Antarctic Peninsula while interannual variability appears in most stations from mid latitudes to the Antarctic coast (Figure 5a). There are a couple of exceptions. The Bellingshausen Station is located in the middle of a cluster of stations with significant decadal variability, though it lacks the decadal variability

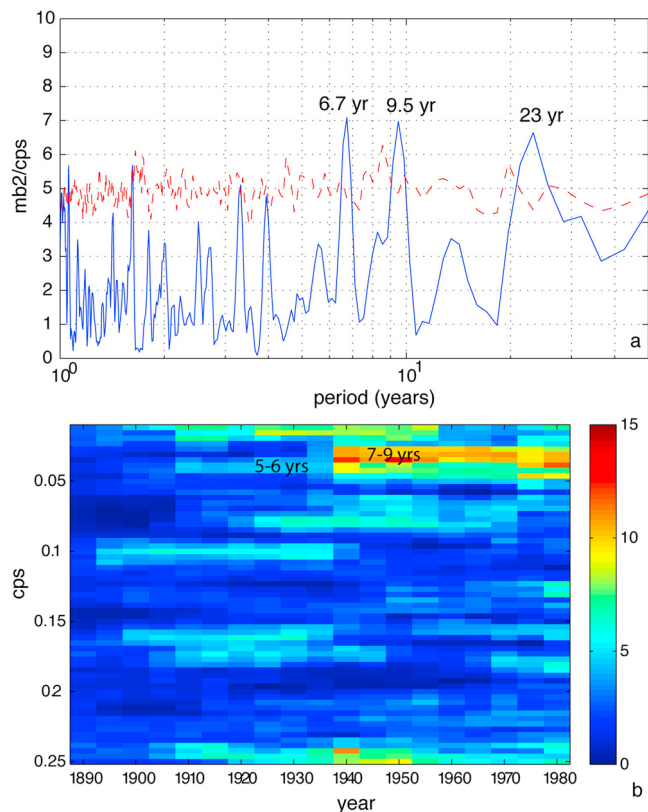


Figure 4. (a) Power spectrum of Fogt's seasonal SAM index (1865–2005) and (b) spectrogram of short time analysis as function of frequency (cycle per season) and center year of each 50-year series. The dash line in Figure 4a indicates the 95% confidence level.

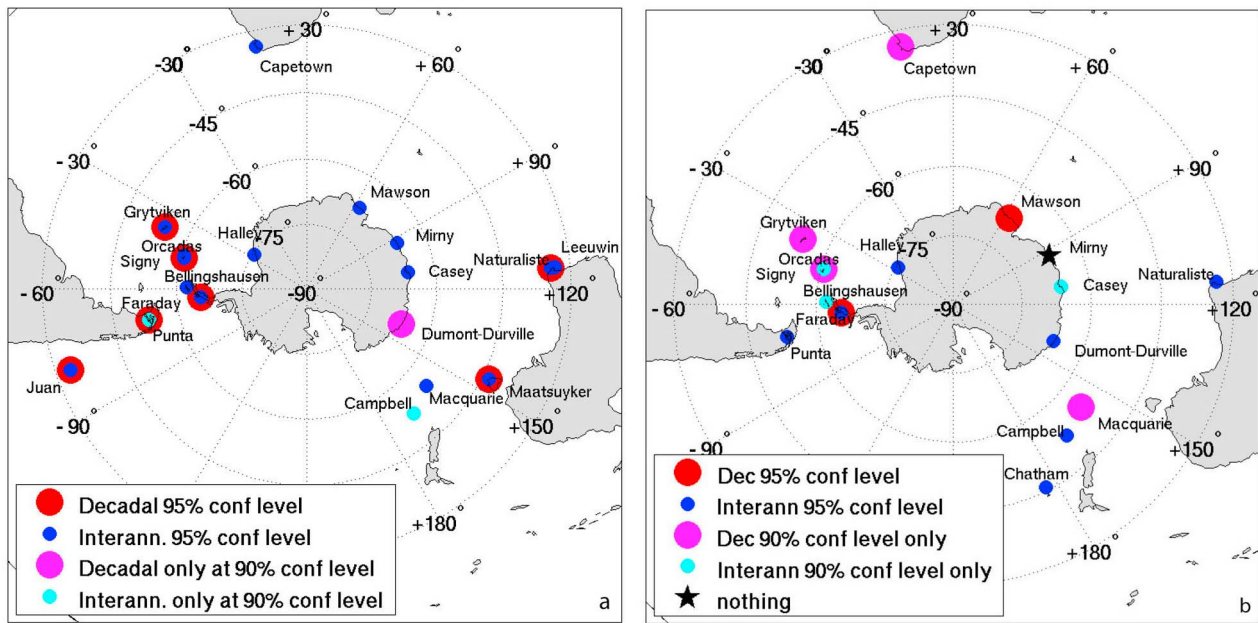


Figure 5. The weather stations with significant interannual (small circles) and decadal (large circles) variability in (a) surface air temperature and (b) SLP in the Southern Ocean.

in both temperature and pressure records. The Campbell Station situated south of New Zealand also lacks of the decadal variability in both temperature and pressure data. Besides these two stations, other stations in mid latitudes and the Antarctic Peninsula exhibit significant decadal variability at least at 90% confidence level (many at 95% confidence level) in either temperature or pressure records,

or in both records. Figure 6 gives an example of temperature spectrogram at Cape Naturaliste where decadal spectra peak at periods of 12–14 years and interannual variability at the period of 4 years are consistent for most time through approximately 100 years records.

[15] To understand the inconsistency of the decadal variability in temperature and SLP at the same location, we

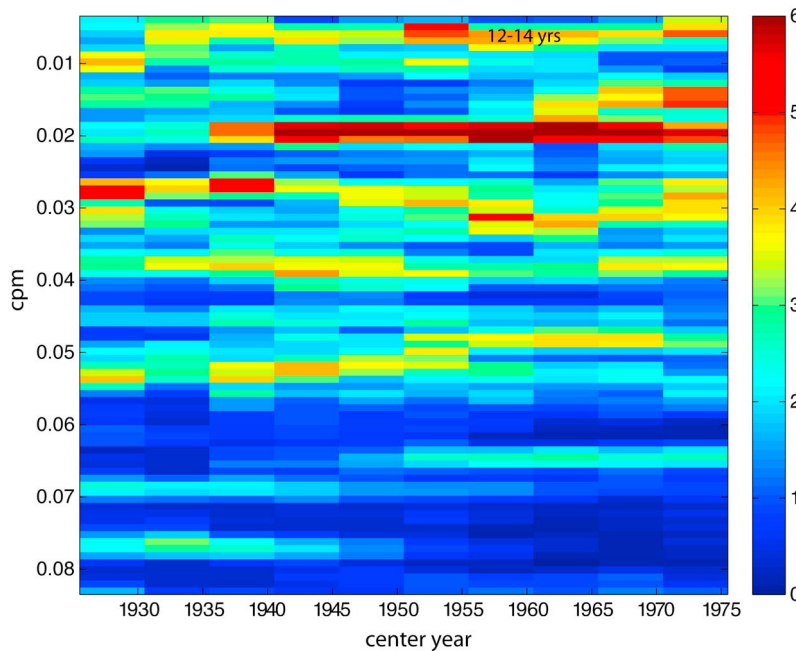


Figure 6. Spectrogram of air temperature at Cape Naturaliste as function of frequency (cycle per month) and center year of each 50-year series.

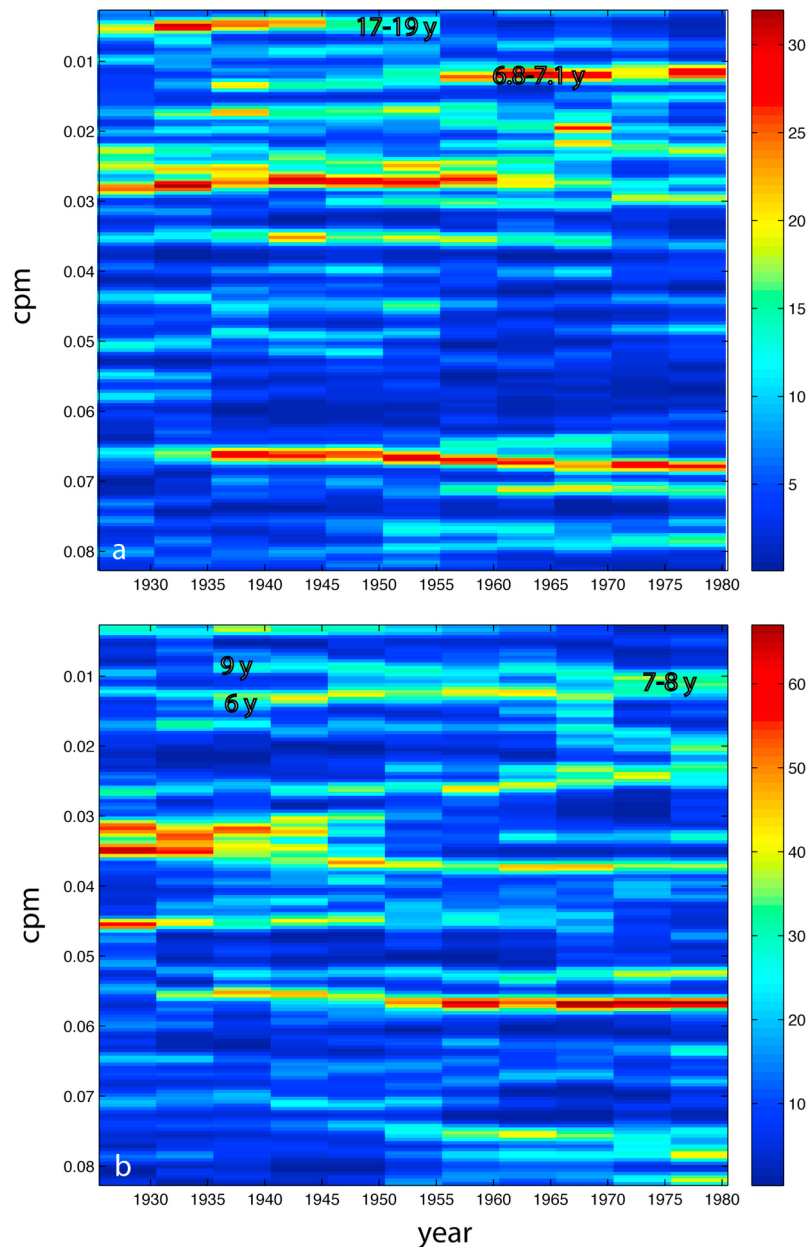


Figure 7. Spectrogram of (a) air temperature and (b) SLP at Orcadas station as function of frequency (cycle per month) and center year of each 50-year series.

give two examples of spectrogram in Figure 7. Air temperature at Orcadas station has a decadal oscillation at period of 17–19 year since 1900 to 1975. The signal disappears after 1970s (Figure 7a). Since the oscillation appears in most of the 100 years series, its spectral peak for the entire series is significant at the 95% confidence level (Figure 5a). On the other hand, pressure records at Orcadas station begin with a decadal variability at a period of 9 years. However, the energy peak quickly shifts toward higher frequency with the period of 6 years to form a broad peak at periods of 7–8 years in later part of the time series (Figure 7b). This energy drift across different frequencies causes the decadal peak in SLP only significant at 90% confidence level

(Figure 5b). It is clear that decadal variabilities in pressure and temperature fields are not necessarily coincide at the same frequency. This may be caused by the data limitation but is more likely caused by differences in thermodynamic and dynamic processes in the atmosphere.

[16] Reanalysis data also capture this natural variability: the zonal mean SLP and air temperature from NCEP/NCAR reanalysis exhibit clear decadal variability in mid latitudes. Contrasting to surface air temperature, the decadal signal in the reanalysis pressure fields becomes even stronger at higher latitudes (not shown here).

[17] To further isolate co-variability in the ocean and atmosphere at the quasi-decadal frequency, we examine temporal variability of SST from 30°S to the subpolar seas

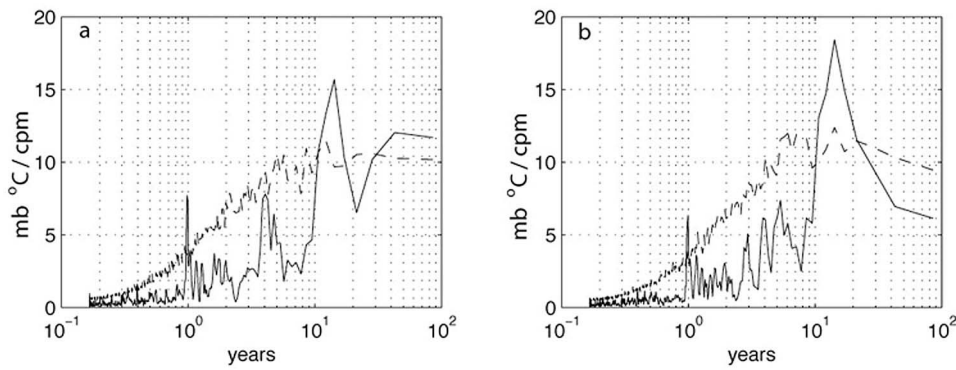


Figure 8. Cross spectrum between SAM index and zonal (a) SST anomaly at 50°S–60°S latitude band and (b) mean meridional SST gradient from 30°S–60°S. The power spectra were smoothed by three-point running mean filter to reduce uncertainty. Dashed line indicates the 95% confidence level.

surrounding Antarctica. First, SST anomaly time series at each grid point is determined by removing its seasonal climatology. These anomaly time series are then zonally averaged around the globe and further averaged into 10 degrees of latitude bands from 30°S to 60°S. Finally, the long-term trend is removed from these series. Power spectrum analysis is applied to these averaged time series. Not surprisingly, decadal peaks are significant at the 95% confidence level in all SST anomaly series (Figures 3b–3d). The decadal periods vary from 11 to 14 years. This result is supported by quasi-decadal changes in the subtropical South Pacific in much shorter time series of SST, salinity and the transport of East

Australia current [Hill *et al.*, 2008], and in satellite observed sea surface height and hydrographic surveys [Qiu and Chen, 2006; Roemmich *et al.*, 2007].

[18] To determine if the decadal variability in the SST field is associated with the decadal variability in the SAM index, we calculate the cross-spectrum analysis between the SAM index and SST anomaly in subpolar seas (50°S to 60°S), as well as with the meridional gradient of SST in mid latitudes from 30°S to 60°S for instrumental periods. Figure 8 shows that both SST in subpolar seas and the mean SST meridional gradient at mid latitudes co-vary with the SAM index at the decadal frequency (14 years).

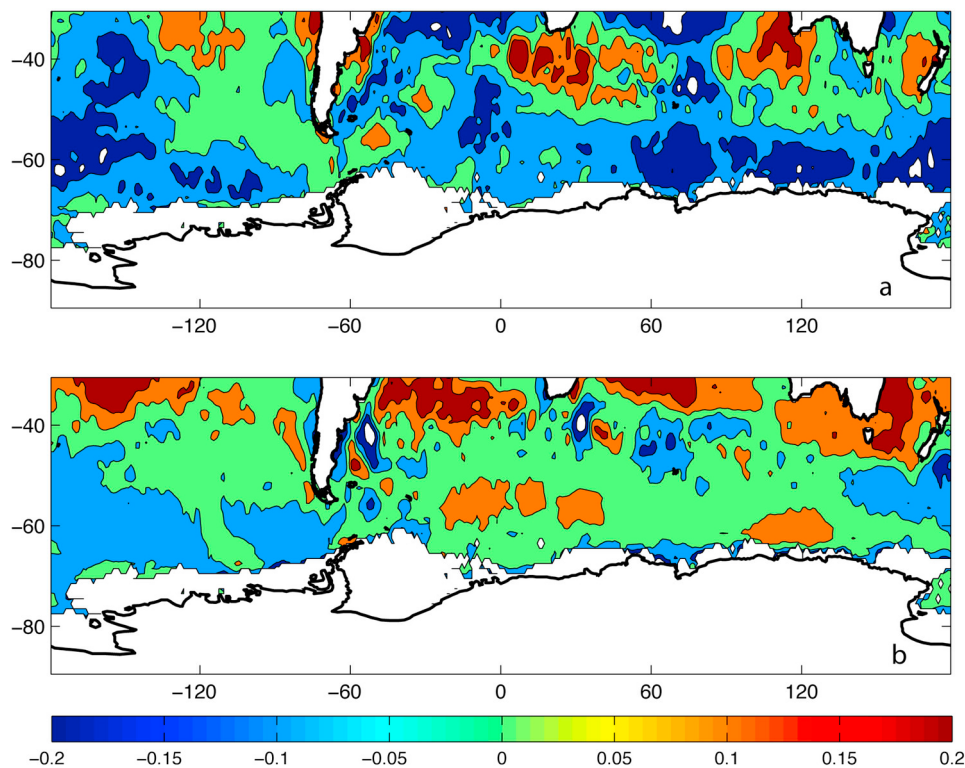


Figure 9. Summer (DJF) composite of SST anomalies for (a) high SAM years (1960–65, 1995–2001) and (b) low SAM decade (1970–80).

Table 3. Decadal Variability in SAM Indices, SST in the 50–60S, and SAM/SST Cross-Spectrum of IPCC Climate Models^a

Country, Institute	Model Name	Time Series	SAM Dec. Var. Period (yrs)	SST 50–60S Dec Var. Period (yrs)	SAM/SST 50–60S Cross-Spec. Per. (yrs)	Ozone Forcing
Canada, CCCMA	cccma_cgcm3.1	1850–2000	8, 9		9, (10)	N
France, CNRM	cnrm_cm3	1860–1999	11,(9)			Y
Australia, CSIRO	csiro_mk3.0	1871–2000	<i>12</i>			Y
USA, NOAA/GFDL	gfdl_cm2.0	1861–2000	<i>8, 10</i>			Y
USA, NOAA/GFDL	gfdl_cm2.1	1861–2000	<i>12</i>			Y
USA, NASA/Goddard	giss_modelE-H	1880–1999	8, 12		8, (11)	Y
USA, NASA/Goddard	giss_modelE-R	1880–2003	12	<i>14</i>	12	Y
China, LASG	iap_fgoals1.0g	1850–1999	<i>10</i>			N
Russia, INM	inmcm3.0	1871–2000	<i>8</i>	<i>8</i>		N
France, PSL	ipsl_cm4	1860–2000	<i>12</i>		<i>11</i>	N
Japan, CCSR,NIES	miroc3.2_hires	1900–2000				Y
Japan, CCSR,NIES	miroc3.2_medres	1850–2000	14		<i>14</i>	Y
Germany, MaxPlan.	mpi_echam5	1860–1999	<i>12</i>	12		Y
Japan, MRI	mri_cgcm2.3.2a	1851–2000	9			N
USA, NCAR	ncar_ccsm3.0	1870–1999	10		<i>11</i>	Y
USA, NCAR	ncar_pcm1	1890–1999	9			Y
UK, Hadley Centre	ukmo_hadcm3	1860–1999	<i>9</i>			Y
UK, Hadley Centre	ukmo_hadgm1	1860–1999		9	10	Y

^aBold (italic) numbers indicate that decadal energy peaks are significant at the 95% (90%) confidence level. Blank spaces indicate no energy peak or that the peak is not significant above 90% confidence level. Presence of ozone forcing in the model is indicated as by *Perlwitz et al.* [2008] and *Lin et al.* [2009].

The result suggests that the midlatitude ocean is a major player in the climate system of the Southern Hemisphere at the decadal time scale.

[19] In addition, we construct a summer SST anomaly composite during two periods of extremely high SAM index and during the decade of 1970–1980 when SAM index is low. SST anomalies in these two composites show clear contrasts, particularly in the center of the South Atlantic, South Indian Ocean and Southwest Pacific. The high SAM years are associated with colder SST in subpolar seas and warmer SST in mid latitudes southwest of Africa and south of Australia (Figure 9a), reflecting a strengthening of meridional temperature gradient across the Antarctic Circumpolar Current (ACC). This pattern is consistent with the mixed layer temperature anomalies associated with positive SAM and can be explained by enhanced Ekman transport and enhanced air-sea heat fluxes associated with stronger westerlies [*Sen Gupta and England, 2006*]. During the low SAM index period, SST in the subtropical gyre (north of 40°S) is warmer than normal and subpolar region of South Atlantic and South Indian Ocean is warmer too (Figure 9b). The SST gradient across ACC would be weakened during the low SAM decades.

5. Decadal Variability in Coupled Climate Models

[20] Instrumental data clearly suggest the existence of decadal variability in mid-high latitudes of the atmosphere and ocean. However, the length of the time series is marginal to draw such conclusions with high statistical confidence. On the other hand, early studies have shown that IPCC AR4 coupled climate models produce a reasonable long term trend in SAM during recent decades [*Cai and Cowan, 2007, Fogt et al., 2009a*]. We, therefore, examine the decadal oscillatory behavior in the twentieth century runs of 18 IPCC climate models (Table 3). All models produce output of over 100 years. *Cai and Cowan* [2007] show that ensemble mean of all models produces the most

realistic trend in SAM. The ensemble mean averages out the natural variability and reveals the net result of climate forcing. However, the decadal variability is a natural variability. Therefore, we choose to construct SAM indices in individual model runs from the models that have multiple runs. It is worth mentioning that all eighteen models produce positive long-term trends in SAM indices, though there is considerable variability in the strength of these trends. Again, all trends are removed. Based on the spectral analysis, significant energy peaks of SAM indices and SST of 50°S–60°S at periods between 8 and 16 years are identified (Table 3). In addition, we also include in the table the energy peaks from the cross spectrum between SAM index and SST at 50°S–60°S of each model. SAM indices in sixteen out of eighteen models yield energy peaks at these decadal frequencies that are significant at least at 90% confidence level (Table 3). If all model runs are considered, 57% of SAM indices yield significant decadal peaks in their spectra. The short time analysis is very supportive to spectra of the entire time series of these models. The decadal peaks at the 95% confidence level usually show consistent energy peak over most of the century or strong peaks for at least half of the century. For example, spectrograms show that the SAM decadal peak at the period of 12 years in GISS E-R model and the peak at the period of 14 years in MIROC3.2 model are consistent through out most of the twentieth century. On the other hands, the decadal peak at the period of 10 years in NCAR CCSM3.0 is more profound in the later half of the twentieth century (not shown here). Many SAM indices in these models have significant decadal peaks at the 95% confidence level over more than 120-year periods (Table 3).

[21] The decadal variability in SST appears in much fewer models. Only four models exhibit significant decadal variability in SST. Eight percent of all model runs produce significant decadal peaks in zonal mean SST. However, there are seven models that display significant decadal peaks in the SAM–SST cross spectrum analysis (Table 3). The less decadal responses in SST raises the question of whether the

AR4 coupled models are able to truly represent the atmosphere-ocean interactions that are relevant to SAM variability at decadal to multidecadal time scales. Recent studies [Meredith and Hogg, 2006; Hogg *et al.*, 2008] suggest that oceanic eddies are important in poleward heat transport in southern high latitudes and eddy kinetic energy increases 2–3 years after a positive peak in the SAM index. Even though the initial SST responses to positive SAM is cooling in high latitudes as shown in Figure 9a, the long-term result is a poleward heat transport by eddies to warm the ocean in high latitudes, particularly south of the polar front. Such a response can only be obtained in eddy resolved models [Screen *et al.*, 2009]. Coarse-resolution climate models are unable to capture this delayed temperature response at low frequencies, which is a possible reason that the SST AR4 model is less responsive to SAM at decadal time scales.

[22] Ozone depletion could be a factor contributing to the increasing trend in SAM during the recent decades [Thompson and Solomon, 2002; Roscoe and Haigh, 2007]. IPCC climate models treat the ozone forcing differently [Perlwitz *et al.*, 2008; Lin *et al.*, 2009]. Studies [Miller *et al.*, 2006; Cai and Cowan, 2007; Fogt *et al.*, 2009a; Karpechko *et al.*, 2010] show that ozone variation is the primary forcing to produce more a realistic trend in SAM during the late twentieth century in climate models. Fogt *et al.* [2009b] reveal that ozone variation impacts the polar atmospheric circulation at intraseasonal time scale. Similarly, increasing of anthropogenic greenhouse gases (GHG) also contributes to the positive trend in SAM [Fyfe *et al.*, 1999; Kushner *et al.*, 2001; Cai *et al.*, 2003; Marshall *et al.*, 2004; Arblaster and Meehl, 2006]. All models we consider here have GHG presence but not every model includes ozone variation. Here we include in Table 3 whether the ozone forcing is used in each climate model. There are no clear relationships between SAM's decadal variability and inclusion of ozone forcing. Therefore, the ozone variability is unlikely a driving force for the natural variability at quasi-decadal time scales.

[23] Considering that these models treat climate forcing differently, the existence of the SAM quasi-decadal variability in most models suggests that it is a natural variability captured by the fundamental physics of climate models.

6. Summary and Discussion

[24] Our analyses of instrumental data document that quasi-decadal oscillatory variability (instead of changes from one decade to next decade) exists in temperature and pressure fields of southern mid-high latitudes, consequently in SAM indices. The multidecadal variability with large amplitude is superimposed on the decadal variability. The results reveal that this quasi-decadal variability is profound in surface air temperature and SLP at weather stations in mid latitudes as well as in zonal mean SST from 30°S to 60°S. In addition, many IPCC climate models exhibit the similar decadal variability in SAM indices in their twentieth century runs with approximately 130 years time series. These results point to one conclusion: a natural variability at quasi-decadal time scales exists in the climate system of the southern ocean. Consistent decadal peaks in SST and in cross-spectra between SAM and SST in observations suggest that the ocean plays an important role at the quasi-decadal time scale. The result is consistent with the oceanic

quasi-decadal variability in the subtropical South Pacific forced by surface winds. This study systematically documents the quasi-decadal variability at the global scale of the Southern Ocean and statistically assesses the robustness of the variability in both the atmosphere and ocean. The results from this study set up a framework within which much regional decadal variability, such as Australian rainfall decadal variability [Meneghini *et al.*, 2007] and decadal variability in the eastern Australian Current [Hill *et al.*, 2008], can be better understood.

[25] Understanding this decadal variability is a very important step to understand the climate system in the southern ocean. Particularly, SAM is a large-scale mode of atmospheric variability and arguably the most significant forcing in the southern hemisphere. Decadal scale changes in SAM, particularly those modulated by multidecadal variability such as the large anomalies in mid 1960s and 1990s, likely act as regime shifts, resulting in different interactions with other climate modes in the Southern Hemisphere. One example is that the impacts from when La Nina and positive SAM were in phase in the 1990s but out of phase in the 1980s resulting in accelerated sea ice retreat west of the Antarctic Peninsula [Stammerjohn *et al.*, 2008]. However, the nature of the SAM-ENSO interaction at this time scale is still not fully understood.

[26] The low frequency variability in SAM should result in changes in the westerlies. The strength and position of maximum wind dictate the ocean ventilation and upwelling, and consequently the meridional overturning circulation. The ocean's responses to changes in westerly winds and SAM have been widely investigated [Hall and Visbeck, 2002; Lovenduski and Gruber, 2005; Sen Gupta and England, 2006; Yang *et al.*, 2007; Sallée *et al.*, 2008]. These studies generally reveal a zonally symmetric Ekman pumping anomaly and Ekman heat transport due to enhanced westerlies. More recently Sallée *et al.* [2010] reveal that the mixed layer depth has a large-scale and zonally asymmetric response to SAM variability at subannual and interannual scales, which are due to the meridional wind associated with the zonally asymmetric pattern of SAM. Our study shows that the magnitude of SAM decadal/multidecadal variability is as large as the total trend over the last 50 years (Figure 2). The potential of SAM/westerlies impact on ocean circulation at this quasi-decadal period cannot be neglected. How much influence that SAM can exert on the overturning circulation at the decadal scale remains unknown and warrants further studies.

[27] **Acknowledgments.** This work is supported by NSF grant ANT 07-39509. E. Yonekura was supported by Climate Center and summer intern program at Lamont-Doherty Earth Observatory of Columbia University in 2006 when she started on this project. Authors appreciate Y. Kushnir's and D. G. Martinson's helpful discussions on spectral significance assessment and short time analysis. Authors appreciate the comments from anonymous reviewers, which help to improve the manuscript greatly. Lamont contribution 7480.

References

- Allan, R. J., and M. R. Haylock (1993), Circulation features associated with the winter rainfall decrease in south-western Australia, *J. Clim.*, *6*, 1356–1367, doi:10.1175/1520-0442(1993)006<1356:CFAWTW>2.0.CO;2.
- Allan, R. J., J. A. Lindesay, and C. J. C. Reason (1995), Multidecadal variability in the climate system over the south-Indian Ocean region

- during the austral summer, *J. Clim.*, *8*, 1853–1873, doi:10.1175/1520-0442(1995)008<1853:MVITCS>2.0.CO;2.
- Arblaster, J. M., and G. A. Meehl (2006), Contributions of external forcings to southern annular mode trends, *J. Clim.*, *19*, 2896–2905, doi:10.1175/JCLI3774.1.
- Bromwich, D. H., A. N. Rogers, P. Kållberg, R. I. Cullather, J. W. C. White, and K. J. Kreutz (2000), ECMWF analyses and reanalyses depiction of ENSO signal in Antarctic precipitation, *J. Clim.*, *13*, 1406–1420, doi:10.1175/1520-0442(2000)013<1406:EAARDO>2.0.CO;2.
- Bromwich, D. H., A. J. Monaghan, and Z. Guo (2004), Modeling the ENSO modulation of Antarctic climate in the late 1990s with the Polar MM5, *J. Clim.*, *17*, 109–132, doi:10.1175/1520-0442(2004)017<0109:MEMOA>2.0.CO;2.
- Bromwich, D. H., R. L. Fogt, K. I. Hodges, and J. E. Walsh (2007), A tropospheric assessment of the ERA-40, NCEP, and JRA-25 global reanalyses in the polar regions, *J. Geophys. Res.*, *112*, D10111, doi:10.1029/2006JD007859.
- Cai, W., and T. Cowan (2007), Trends in Southern Hemisphere circulation in IPCC AR4 models over 1950–99: Ozone depletion versus greenhouse forcing, *J. Clim.*, *20*, 681–693, doi:10.1175/JCLI4028.1.
- Cai, W., P. H. Whetton, and D. J. Karoly (2003), The response of the Antarctic Oscillation to increasing and stabilized atmospheric CO₂, *J. Clim.*, *16*, 1525–1538, doi:10.1175/1520-0442-16.10.1525.
- Cullather, R. I., D. H. Bromwich, and M. L. vanWoert (1996), Interannual variations in Antarctic precipitation related to El Niño–Southern Oscillation, *J. Geophys. Res.*, *101*, 19,109–19,118, doi:10.1029/96JD01769.
- Fogt, R. L., and D. H. Bromwich (2006), Decadal variability of the ENSO teleconnection to the high-latitude South Pacific governed by coupling with the Southern Annular Mode, *J. Clim.*, *19*, 979–997, doi:10.1175/JCLI3671.1.
- Fogt, R. L., J. Perlwitz, A. J. Monaghan, D. H. Bromwich, J. M. Jones, and G. J. Marshall (2009a), Historical SAM variability. Part II: Twentieth-century variability and trends from reconstructions, observations, and the IPCC AR4 models, *J. Clim.*, *22*, 5346–5365, doi:10.1175/2009JCLI2786.1.
- Fogt, R. L., J. Perlwitz, S. Pawson, and M. A. Olsen (2009b), Intra-annual relationships between polar ozone and the SAM, *Geophys. Res. Lett.*, *36*, L04707, doi:10.1029/2008GL036627.
- Fyfe, J. C., G. J. Boer, and G. M. Flato (1999), The Arctic and Antarctic oscillations and their projected changes under global warming, *Geophys. Res. Lett.*, *26*(11), 1601–1604.
- Gong, D., and S. Wang (1999), Definition of Antarctic Oscillation index, *Geophys. Res. Lett.*, *26*, 459–462, doi:10.1029/1999GL900003.
- Hall, A., and M. Visbeck (2002), Synchronous variability in the Southern Hemisphere atmosphere, sea ice, and ocean resulting from the annular mode, *J. Clim.*, *15*(21), 3043–3057, doi:10.1175/1520-0442(2002)015<3043:SVITSH>2.0.CO;2.
- Hill, K. L., S. R. Rintoul, E. R. Coleman, and K. R. Ridgway (2008), Wind forced low frequency variability of the East Australia Current, *Geophys. Res. Lett.*, *35*, L08602, doi:10.1029/2007GL032912.
- Hogg, A. M., M. P. Meredith, J. R. Blundell, and C. Wilson (2008), Eddy heat flux in the Southern Ocean: Response to variable wind forcing, *J. Clim.*, *21*, 608–620, doi:10.1175/2007JCLI1925.1.
- Hurrell, J. W., J. J. Hack, D. Shea, J. M. Caron, and J. Rosinski (2008), A new sea surface temperature and sea ice boundary dataset for the Community Atmosphere Model, *J. Clim.*, *21*, 5145–5153, doi:10.1175/2008JCLI2292.1.
- Jones, J. M., R. L. Fogt, M. Widmann, G. J. Marshall, P. D. Jones, and M. Visbeck (2009), Historical SAM variability. Part I: Century length seasonal reconstructions, *J. Clim.*, *22*, 5319–5345, doi:10.1175/2009JCLI2785.1.
- Kalnay, E., et al. (1996), The NCEP/NCAR 40-year reanalysis project, *Bull. Am. Meteorol. Soc.*, *77*, 437–471, doi:10.1175/1520-0477(1996)077<0437:TNYRP>2.0.CO;2.
- Karpechko, A. Y., N. P. Gillett, L. J. Gray, and M. Dall'Amico (2010), Influence of ozone recovery and greenhouse gas increases on Southern Hemisphere circulation, *J. Geophys. Res.*, *115*, D22117, doi:10.1029/2010JD014423.
- Kidson, J. W. (1999), Principal modes of Southern Hemisphere low frequency variability obtained from NCEP–NCAR reanalyses, *J. Clim.*, *12*, 2808–2830, doi:10.1175/1520-0442(1999)012<2808:PMOSHL>2.0.CO;2.
- Kistler, R., et al. (2001), The NCEP–NCAR 50-year reanalysis: Monthly means CD-ROM and documentation, *Bull. Am. Meteorol. Soc.*, *82*, 247–267, doi:10.1175/1520-0477(2001)082<0247:TNNYRM>2.3.CO;2.
- Kushner, P. J., I. M. Held, and T. L. Delworth (2001), Southern Hemisphere atmospheric circulation response to global warming, *J. Clim.*, *14*, 2238–2249, doi:10.1175/1520-0442(2001)014<0001:SHACT>2.0.CO;2.
- Lin, P., Q. Fu, S. Solomon, and J. M. Wallace (2009), Temperature trend patterns in Southern Hemisphere high latitudes: Novel indicators of stratospheric change, *J. Clim.*, *22*, 6325–6341, doi:10.1175/2009JCLI2971.1.
- Lovenduski, N. S., and N. Gruber (2005), Impact of the Southern Annular Mode on Southern Ocean circulation and biology, *Geophys. Res. Lett.*, *32*, L11603, doi:10.1029/2005GL022727.
- Marshall, G. J. (2003), Trends in the Southern Annular Mode from observations and reanalyses, *J. Clim.*, *16*, 4134–4143, doi:10.1175/1520-0442(2003)016<4134:TITSAM>2.0.CO;2.
- Marshall, G. J., P. A. Stott, J. Turner, W. M. Connolley, J. C. King, and T. A. Lachlan-Cope (2004), Causes of exceptional atmospheric circulation changes in the Southern Hemisphere, *Geophys. Res. Lett.*, *31*, L14205, doi:10.1029/2004GL019952.
- Meneghini, B., I. Simmonds, and I. N. Smith (2007), Association between Australian rainfall and the Southern Annular Mode, *Int. J. Climatol.*, *27*, 109–121, doi:10.1002/joc.1370.
- Meredith, M. P., and A. M. Hogg (2006), Circumpolar response of Southern Ocean eddy activity to a change in the Southern Annular Mode, *Geophys. Res. Lett.*, *33*, L16608, doi:10.1029/2006GL026499.
- Miller, R. L., G. A. Schmidt, and D. T. Shindell (2006), Forced annular variations in the 20th century Intergovernmental Panel on Climate Change Fourth Assessment Report models, *J. Geophys. Res.*, *111*, D18101, doi:10.1029/2005JD006323.
- Perlwitz, J., S. Pawson, R. L. Fogt, J. E. Nielsen, and W. D. Neff (2008), Impact of stratospheric ozone hole recovery on Antarctic climate, *Geophys. Res. Lett.*, *35*, L08714, doi:10.1029/2008GL033317.
- Pittock, A. B. (1980), Patterns of climatic variation in Argentina and Chile. I. Precipitation, 1931–1960, *Mon. Weather Rev.*, *108*, 1347–1361, doi:10.1175/1520-0493(1980)108<1347:POCVIA>2.0.CO;2.
- Priestley, M. B. (1992), *Spectral Analysis and Time Series*, Academic, London.
- Qiu, B., and S. Chen (2006), Decadal variability in the large scale sea surface height field of the South Pacific Ocean: Observations and causes, *J. Phys. Oceanogr.*, *36*(9), 1751–1762, doi:10.1175/JPO2943.1.
- Rayner, N. A., D. E. Parker, E. B. Horton, C. K. Folland, L. V. Alexander, D. P. Rowell, E. C. Kent, and A. Kaplan (2003), Global analyses of sea surface temperature, sea ice, and night marine air temperature since the late nineteenth century, *J. Geophys. Res.*, *108*(D14), 4407, doi:10.1029/2002JD002670.
- Reason, C. J. C. (2000), Multidecadal climate variability in the subtropics/mid-latitudes of the Southern Hemisphere oceans, *Tellus, Ser. A*, *52*, 203–223.
- Roemmich, D., J. Gilson, R. Davis, P. Sutton, S. Wijffels, and S. Riser (2007), Decadal spin up of the subtropical gyre in the South Pacific, *J. Phys. Oceanogr.*, *37*, 162–173, doi:10.1175/JPO3004.1.
- Rogers, J. C., and H. van Loon (1982), Spatial variability of sea-level pressure and 500 mb height anomalies over the Southern Hemisphere, *Mon. Weather Rev.*, *110*(10), 1375–1392, doi:10.1175/1520-0493(1982)110<1375:SVOSLP>2.0.CO;2.
- Roscoe, H. K., and J. D. Haigh (2007), Influences of ozone depletion, the solar cycle and the QBO on the Southern Annular Mode, *Q. J. R. Meteorol. Soc.*, *133*, 1855–1864, doi:10.1002/qj.153.
- Salinger, M. J., R. J. Allan, N. Bindoff, J. Hannah, B. Lavery, Z. Lin, J. A. Lindesay, N. Nicholls, N. Plummer, and S. Torok (1996), Observed variability and change in climate and sea level in Australia, New Zealand and the South Pacific, in *Greenhouse—Coping With Climate Change*, edited by W. J. Bouma, G. I. Pearman, and M. R. Manning, pp. 100–126, CSIRO Publ., Collingwood, Victoria, Australia.
- Sallée, J. B., K. G. Speer, and R. Morrow (2008), Response of the Antarctic Circumpolar Current to atmospheric variability, *J. Clim.*, *21*, 3020–3039, doi:10.1175/2007JCLI1702.1.
- Sallée, J. B., K. G. Speer, and S. R. Rintoul (2010), Zonally asymmetric response of the Southern Ocean mixed-layer depth to the Southern Annular Mode, *Nat. Geosci.*, *3*, 273–279, doi:10.1038/ngeo812.
- Screen, J. A., N. P. Gillett, D. P. Stevens, G. J. Marshall, and H. K. Roscoe (2009), The role of eddies in the Southern Ocean temperature response to the Southern Annular Mode, *J. Clim.*, *22*, 806–818, doi:10.1175/2008JCLI2416.1.
- Sen Gupta, A., and M. H. England (2006), Coupled ocean–atmosphere–ice response to variations in the Southern Annular Mode, *J. Clim.*, *19*, 4457–4486, doi:10.1175/JCLI3843.1.
- Simmonds, I. (2003), Modes of atmospheric variability over the Southern Ocean, *J. Geophys. Res.*, *108*(C4), 8078, doi:10.1029/2000JC000542.
- Simmonds, I., and J. C. King (2004), Global and hemispheric climate variations affecting the Southern Ocean, *Antarct. Sci.*, *16*, 401–413, doi:10.1017/S0954102004002226.

- Stammerjohn, S. E., D. G. Martinson, R. C. Smith, X. Yuan, and D. Rind (2008), Trends in Antarctic sea ice spring retreat and autumn advance in response to ENSO and Southern Annular Mode Variability, *J. Geophys. Res.*, *113*, C03S90, doi:10.1029/2007JC004269.
- Thompson, D. W. J., and S. Solomon (2002), Interpretation of recent Southern Hemisphere climate changes, *Science*, *296*, 895–899, doi:10.1126/science.1069270.
- Thompson, D. W. J., and J. M. Wallace (2000), Annular modes in the extratropical circulation, part I, Month-to-month variability, *J. Clim.*, *13*, 1000–1016, doi:10.1175/1520-0442(2000)013<1000:AMITEC>2.0.CO;2.
- Turner, J., S. R. Colwell, G. J. Marshall, T. A. Lachland-Cope, A. M. Carleton, P. D. Jones, V. Lagun, P. A. Reid, and S. Iagovkina (2005), Antarctic climate change during the last 50 years, *Int. J. Climatol.*, *25*, 279–294, doi:10.1002/joc.1130.
- Turner, J., J. C. Comiso, G. J. Marshall, T. A. Lachlan-Cope, T. Bracegirdle, T. Maksym, M. P. Meredith, Z. M. Wang, and A. Orr (2009), Non-annular atmospheric circulation change induced by stratospheric ozone depletion and its role in the recent increase of Antarctic sea ice extent, *Geophys. Res. Lett.*, *36*, L08502, doi:10.1029/2009GL037524.
- Uppala, S. M., et al. (2005), The ERA-40 Reanalysis, *Q. J. R. Meteorol. Soc.*, *131*, 2961–3012, doi:10.1256/qj.04.176.
- Venegas, S. A., L. A. Mysak, and D. N. Straub (1996), Evidence for inter-annual and interdecadal climate variability in the South Atlantic, *Geophys. Res. Lett.*, *23*, 2673–2676, doi:10.1029/96GL02373.
- Villalba, R., E. R. Cook, R. D. D. Ö. Arrigo, G. C. Jacoby, and P. D. Jones (1997), Sea-level pressure variability around Antarctica since A.D. 1750 inferred from subantarctic tree-ring records, *Clim. Dyn.*, *13*, 375–390, doi:10.1007/s003820050172.
- Visbeck, M. (2009), A station-based Southern Annular Mode index from 1884 to 2005, *J. Clim.*, *22*, 940–950, doi:10.1175/2008JCLI2260.1.
- Yang, X. Y., D. X. Wang, J. Wang, and R. X. Huang (2007), Connection between the decadal variability in the Southern Ocean circulation and the Southern Annular Mode, *Geophys. Res. Lett.*, *34*, L16604, doi:10.1029/2007GL030526.
- Yuan, X., and C. Li (2008), Climate modes in southern high latitudes and their impacts on Antarctic sea ice, *J. Geophys. Res.*, *113*, C06S91, doi:10.1029/2006JC004067.

E. Yonekura, Department of Earth and Environmental Sciences, Columbia University, New York, NY 10027, USA.

X. Yuan, Lamont-Doherty Earth Observatory of Columbia University, 61 Rt. 9W, Palisades, NY 10964, USA. (xyuan@ldeo.columbia.edu)